Microfluidics and Nanofluidics (2021) 25:77
https://doi.org/10.1007/s10404-021-02479-y

RESEARCH PAPER

A simple approach to fabricate multi-layer glass microfluidic chips based on laser processing and thermocompression bonding

Yong Han[1,2,3] · Zeheng Jiao[1,2,3] · Jingjing Zhao[4] · Zixi Chao[1,2,3] · Zheng You[1,2,3]

Received: 21 June 2021 / Accepted: 5 August 2021 / Published online: 16 August 2021
© The Author(s), under exclusive licence to Springer-Verlag GmbH Germany, part of Springer Nature 2021

Abstract

Glass is an ideal material for microfluidic chips because of its pressure resistance, chemical stability, optical transparency, and thermal stability. Two-layer or three-layer microfluidic glass chips, composed of one or two cover layers and one structural layer, have been widely applied to two-dimensional microfluidic systems. Due to the fabrication difficulties in aligning and bonding multiple glass layers, multi-layer glass chips (more than three layers) are underutilized, although they are essential to deliver more complicated microfluidic functionalities and achieve more accurate microfluidic manipulations. This work proposes a fabrication process based on rapid laser cutting of single glass layers and one-time thermocompression bonding of multi-layer chips and demonstrated it with a five-layer microfluidic chip for three-dimensional (3D) hydrodynamic focusing. The pressure and temperature are the key parameters for multi-layer bonding, which are experimentally determined to be 0.4 MPa and 605 ℃. Five-layer glass microfluidic chips could be fabricated within 6 h with a bonding strength of 0.6 MPa. This simple, easy-to-operate fabrication method for the rapid production of multi-layer glass microfluidic chips will be conducive to the wide application of multi-layer microfluidic glass chips.

Keywords Multi-layer · Microfluidics chip · Laser processing · Thermocompression bonding

1 Introduction

Benefiting from the high chemical stability (Webb et al. 1976), optical transparency from ultraviolet to infrared (Kitamura et al. 2007), and biocompatibility (Hwang et al. 2019), glass is an ideal material for microfluidic chips (Daridon et al. 2001; Jiao et al. 2019; Kim et al. 2019). According to the structural complexity, microfluidic chips can be divided into two groups: two-layer or three-layer chips for 2D microfluidic systems (Sung-Il et al. 2018) and multi-layer chips for 3D microfluidic systems (Chen et al. 2016). Two-layer or three-layer microfluidic chips usually consist of a functional layer with micro-channels and one or two cover plates to seal the chip. However, in many cases such as cell culturing (Jang and Suh 2010), sample mixing (Lee et al. 2011; Xiong and Chen 2021a, b; Xiong and Chen 2021a, b; Xiong et al. 2021), and 3D sample focusing (Zhao and You 2015; Wu et al. 2018), two or three-layer microfluidic chip cannot achieve ideal performance without increasing the number of layers to form more complicated 3D micro-structures.

Although 3D microfluidic chips are capable of providing more complicated microfluidics functionalities, the fabrication of multi-layer glass microfluidic chips is a real challenge due to the chemical and physical inert of glass material, limiting the applications of 3D microfluidic glass chips. The multi-layer microfluidic chips reported are usually fabricated by complicated, costly, and time-consuming processes. Currently, most multilayer microfluidic devices are made of polymethylmethacrylate (PMMA) or polydimethylsiloxane (PDMS). For example, multi-layer PMMA chips could be fabricated using laser cutting and plasma-activated thermal bonding (Li et al. 2009), and multi-layer PDMS chips

✉ Jingjing Zhao
zhaojj@stanford.edu

✉ Zheng You
yz-dpi@mail.tsinghua.edu.cn

1 State Key Laboratory of Precision Measurement Technology and Instrument, Tsinghua University, Beijing 100084, China

2 Department of Precision Instrument, Tsinghua University, Beijing 100084, China

3 Beijing Laboratory for Biomedical Detection Technology and Instrument, Tsinghua University, Beijing 100084, China

4 Department of Structural Biology, Stanford University, School of Medicine, Stanford, CA 94305-5126, USA

could be produced with soft lithography and plasma bonding (Moraes et al. 2009; Wu et al. 2011). Regardless of the material, the current multi-layer microfluidic chip is generally composed of two steps: single-layer processing and multi-layer bonding (Liu et al. 2021).

The first step is to fabricate microstructures on each glass layer. Wet etching is an isotropic processing method for glass by using the solution of hydrofluoric acid with the etching rate below 10 μm/min (Iliescu et al. 2005, 2008). Dry etching is an anisotropic process performed in deep reactive ion etching reactors (Park et al. 2005) and its etching rate is around 0.5–0.7 μm/min, which is more suitable for fine structures with the feature size from sub-micro to several microns. Both the above etching methods require the etched material to be patterned with an etch-resistant layer by lithography (Iliescu et al. 2012). Computer numerical control (CNC) micromachining utilizes micro grinding-tools to carve microstructures on glass plates (Jin et al. 2020). Since glass is brittle, CNC machining is a highly demanding expertise. Laser processing is the fastest processing method, based on short nanosecond or picosecond laser pulses, and can easily pattern more than 10 μm of depth with a supreme sidewall verticality (Adam et al. 2015; Gečys et al. 2015). Since microfluidic chips are often used for cell or droplet manipulation (Chen et al. 2020; Yang et al. 2021), the feature size of the chip structure is usually on the order of 10^1–10^2 μm, which is within the capabilities of laser processing.

The second step is to bond multiple glass layers together. Due to the difficulties in the precise alignment and the sufficient bonding of multiple glass plates, the bonding step suffers from the complex process, cumbersome manual operation, and low productivity. The common glass bonding methods include anodic bonding that is performed at high temperature and voltage (Berthold et al. 2000; Mrozek 2012), surface pretreated bonding that uses a complex cleaning process, and physical or chemical process to pretreat the glass surface to change the surface properties to bond the glass in mild conditions (Jia et al. 2004; Iles et al. 2007; Xu et al. 2013; Sano et al. 2020), thermocompression bonding that heats the glass to the annealing point temperature and applies pressure to fuse the glass (Akiyama et al. 2007; Kalkowski et al. 2014), adhesive bonding that utilizes UV curable adhesive to bond different layers (Pan and Yang 2006; Su et al. 2019), and laser bonding where the laser is used to heat the interfaces to complete local bonding of two substrates (Du and Allen 2018, 2019). However, the previous researches mainly focus on the bonding of two glass layers and could not be directly used for multi-layer microfluidic glass chips. For anodic bonding, an additional conductive intermediate layer such as Ti (Mrozek 2009) or amorphous silicon (Datta et al. 2006) is required between glass substrates, not only making the bonding of multiple glass layers complicated but also reducing the transparency of the glass chip. For surface pre-treatment bonding, the treatment process is time-consuming and requiring considerable expertise, for example, 8–12 h of concentrated sulfuric acid soak (Jia et al. 2004) or O_2/CF_4 plasma treatment (Xu et al. 2013) are used to activate the glass surface. In addition, the alignment between the pretreated glass layers also needs to be very careful to avoid introducing impurities, it is difficult to bond the multi-layer glass at one time. In adhesive bonding, the adhesive material must be well controlled to avoid flowing into the microfluidics channel, which is highly dependent on the operator's skills, especially when there are more than three layers of glass (Iliescu et al. 2012). Laser bonding is suitable for single interface bonding with small areas, and it is difficult to control laser focusing for multi-layer bonding because the laser should precisely focus on the interfaces of two adjacent glass layers.

Aiming to solve the difficulties in the fabrication of multi-layer microfluidic glass chips, we combine laser cutting and thermocompression bonding to develop a simple multi-layer glass bonding technique. Laser processing is adopted considering the efficiency and accuracy of fabrication while thermocompression bonding is able to bond multiple glass surfaces at one time after the glass plates are accurately aligned. We used a five-layer 3D microfluidics chip (Zhao and You 2016) to validate the fabrication process. The chip is composed of 5 layers of glass and the structure on each layer is etched by a picosecond laser matching machine. After simple cleaning and one-time alignment operation, the chip is placed in a vacuum thermocompression bonding machine for one-time bonding. The entire manufacturing process is carried out in a normal room environment without requiring a cleanroom environment, and manual operations are only involved in cleaning and alignment. Using the above method, the five-layer glass microfluidic chip can be manufactured within 6 h. Tensile tests and sealing tests were performed to evaluate the boding quality of the chips. Chips bonded at different temperatures and UV adhesive-bonded chips were tested using a tensile machine to compare the bonding strengths, and the hydrodynamic focusing of the chips was characterized by confocal imaging. In brief, this fabrication technology can produce multi-layer glass microfluidic chips in five steps of laser cutting, glass cleaning, chip alignment, bonding, and cooling.

2 Materials and methods

2.1 Materials

The chip is made from rectangular Asahi float glass (Asahi Glass, Japan) plates with the size of 4 cm × 6 cm. As shown in Fig. 1(c), the glass chip is composed of five layers, two

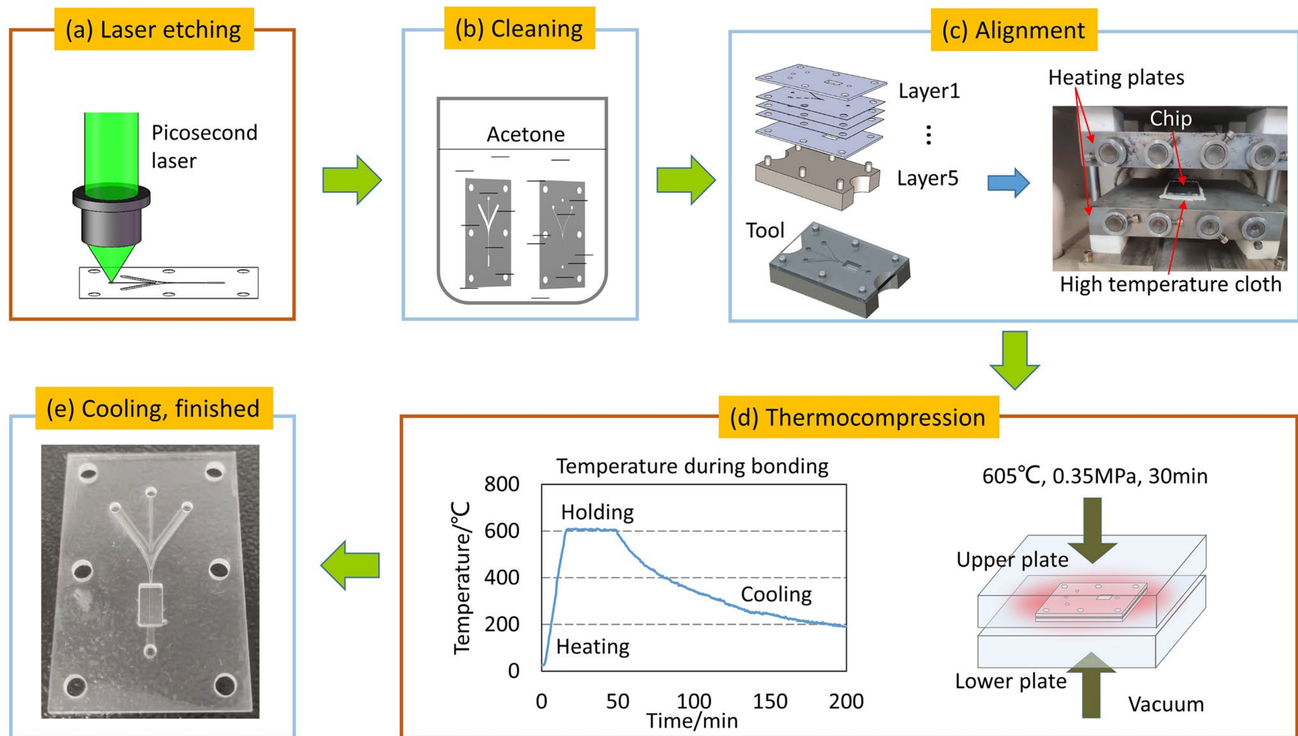

Fig. 1 The process of 5-layer glass microfluidic chip fabrication based on laser processing and thermocompression

1 mm thick glass as the cover plates, and three 165 µm thin layers with flow channels as the middle layers. Three middle thin layers complete 3D hydrodynamic focusing, and the upper and lower layers are used to seal the chip, which is introduced in detail in our previous works (Zhao and You 2015, 2016, 2018).

2.2 Methods

Figure 1 illuminates that the whole process is composed of five parts: laser processing, glass cleaning, chip alignment, thermocompression bonding, and cooling.

2.3 Laser processing

The first step is laser processing. A picosecond laser micromachining machine (Delphi laser, Suzhou, China) is used to directly transfer the design onto a single glass layer by cutting through the glass substrates. The 532 nm green laser works in pulse mode, with the maximum laser power of 15 W. The focused laser size is 15 µm ($1/e^2$) and the depth-of-focus is around 150 µm. The laser spot is controlled by the Galvo mirror to move transversely and laterally at the speed of 200 mm/s to etch channels and structures on the glass sheets. For the 1 mm thick glass plates, the laser spot is moved axially into the glass with a step of 12 µm to repeatedly etch the glass plates. After about 85 times of repeated etching, the thick glass plate can be cut through with the designed structures. For 165 µm glass layer, only one etching is needed to cut through the glass sheet. The laser pulse repetition rate is 67 kHz with 80% duty factor for 1 mm glass and 40 kHz with 99% duty factor for 165 µm glass layers. The average laser power for 165 µm and 1 mm glass layers are 2.5 W and 3.6 W respectively. The fabrication error of the channel dimension is 5 µm, and the size of the laser ablation edge is 5 µm. In general applications, the roughness of the sidewall could be improved by reducing the laser power and the laser scanning speed (Huang et al. 2010). The time of laser processing depends on the thickness of the glass sheet and the total length of the processed pattern. For the chip shown in Fig. 1(c), it takes 15 min to process three 165 µm thin glass sheets and 80 min to process two 1 mm thick glass sheets. All five layers of glass are processed within 95 min.

2.4 Glass cleaning

After the structures are fabricated on the glass sheets, the second step is to clean the glass. Glass cleaning is to remove impurities on the surface of the glass, such as dust and fingerprints, providing clean and flat surfaces for the glass bonding. The cleaning procedure in Fig. 1(b) comprises four sub-steps. The first is an acetone ultrasonic bath for 3 min to dissolve the organic impurities on the surface. The second is to use lint-free paper (KW32, Kimwipe, GA, USA) to dry

the glass surfaces. The third step is 3 min ultrasonic cleaning with anhydrous ethanol to dissolve the contaminants and residual acetone. The last is to dry the glass plates naturally in the fume hood. After cleaning, it should not be able to see any stains or particles on the glass surface by microscope detection. Otherwise, repeat the above cleaning steps.

2.5 Chip alignment

The third step is the alignment between multiple layers of glass, which is also important to the function of the chip. The misalignment of different layers will change the 3D structures of the flow channel, adversely affecting the fluid dynamics in the chip. The actual performance of the chip will deviate from the design. For instance, the 3D dynamic focusing chips developed in our previous works (Zhao and You 2015, 2016) require that the three middle layers are aligned accurately with the error less than 10 μm to ensure the symmetry of the flow channel and the focusing performance. Six positioning holes with the 4 mm diameter are fabricated around the edge of each glass sheet, corresponding to the 6 pillars of the same size on the alignment tool. Five layers of glass are put on the tool at one time, tested by the microscope, the position errors are usually less than 10 μm. Followed by the alignment, a small amount of deionized water is used to infiltrate the thin gaps between two adjacent glass sheets. The Van der Waals force between the water molecules and the glass surface can prevent the glass sheets from shifting and keep the relative positions of the glass sheets constant.

2.6 Thermocompression bonding and cooling

The last two steps are bonding and cooling. The basic principle of thermocompression bonding is to heat the glass to a temperature above the annealing point and then apply pressure to fuse the glass layers. The ideal pressure of ~ 0.4 MPa and the temperature of ~ 605 ℃ are determined via a series of experiments in this work. After thermocompression, the two adjacent glass sheets are fused together and might deform slightly. The bonding is operated with a customized machine (JKD-TH018III, Shenzhen Jingkeda, China), and its physical diagram is shown in Fig. 1(c). The upper and lower heating plates can be heated up to 800 ℃ and offer a maximum force of 1.9kN. The pressure between the plates is controlled by an air cylinder whose input air pressure is adjusted between 0 and 0.6 MPa). During the bonding, two pieces of flexible high-temperature resistant cloth are placed between the glass chip and the heat plate to homogenize the pressure, pressing the chip evenly. The heater temperature is precisely controlled by the computer closed-loop system and the temperature curve is shown in Fig. 1(d). First, the plates are gradually heated to 605 °C at a rate of 40 °C/min. When it is at the target temperature, the two plates start to apply a force of 1000 N on the microfluidic chip (equivalent to a pressure of 0.4 MPa). Second, the heating plates are kept at 605 °C for 30 min to fuse the glass plates, then the heating process is stopped. Third, after 2.5 h of cooling, the chip is cooled down to below 200 °C, and will be taken out from the chamber and naturally cools down in the air. During the entire heating and cooling process, the cavity of the bonding machine is evacuated into a vacuum environment (23 mbar) to prevent oxidation of the heating plates. To speed up the cooling process, the inner wall of the cavity uses water cooling. The temperature is the most important factor in the thermocompression process, at 605℃, the five-layer chip has a relatively high bonding strength and small channel deformation. The temperature effect is further elaborated in the Sect. 3.

3 Experiments and results

In this part, the bonding strength, channel deformation, sealing performance, and microfluidic function of the multilayer chip were tested to evaluate the fabrication quality.

3.1 Bonding strengths tests

The bonding strength is an important characterization of chip quality, which is related to bonding temperature (Akiyama et al. 2007). To determine the optimal bonding temperature, we examined the chips bonded at seven different temperatures in the range of 580–610 °C. The bonding strength was measured by a tensile testing machine (ZWICKZ020, Germany, ZWICK, the maximum tensile force = 20kN). Figure 2(a) shows the setup of the tensile test, the five-layer chip was glued on a T-shaped mold made of Q235B steel using metal glue (JL-109, China, JuLi). The testing machining worked at speed of 1 mm/min, and the maximum tensile force was recorded. In addition, the bonding strength of UV-curable adhesive chip was measured for comparison.

The strength curve is shown in Fig. 2(b), and the real chips for test are shown in Fig. 2(d). When the temperature is low (< 600 ℃), the glass is not softened enough, the bonding area and bonding strength between the layers is insufficient. But when the temperature reaches a critical value (> 600 ℃), the bonding strength rises sharply with an apparent increment in the fused area, as shown in Fig. 2(c). When the temperature is over 620℃, the glass chip begins to adhere to the upper heating plate, and the deformation of the glass structure becomes unacceptable. Considering the above factors, the optimal bonding temperature is determined at 605 ℃, generating a bonding strength of 0.6 MPa. It is stronger than the strength of the adhesive chip.

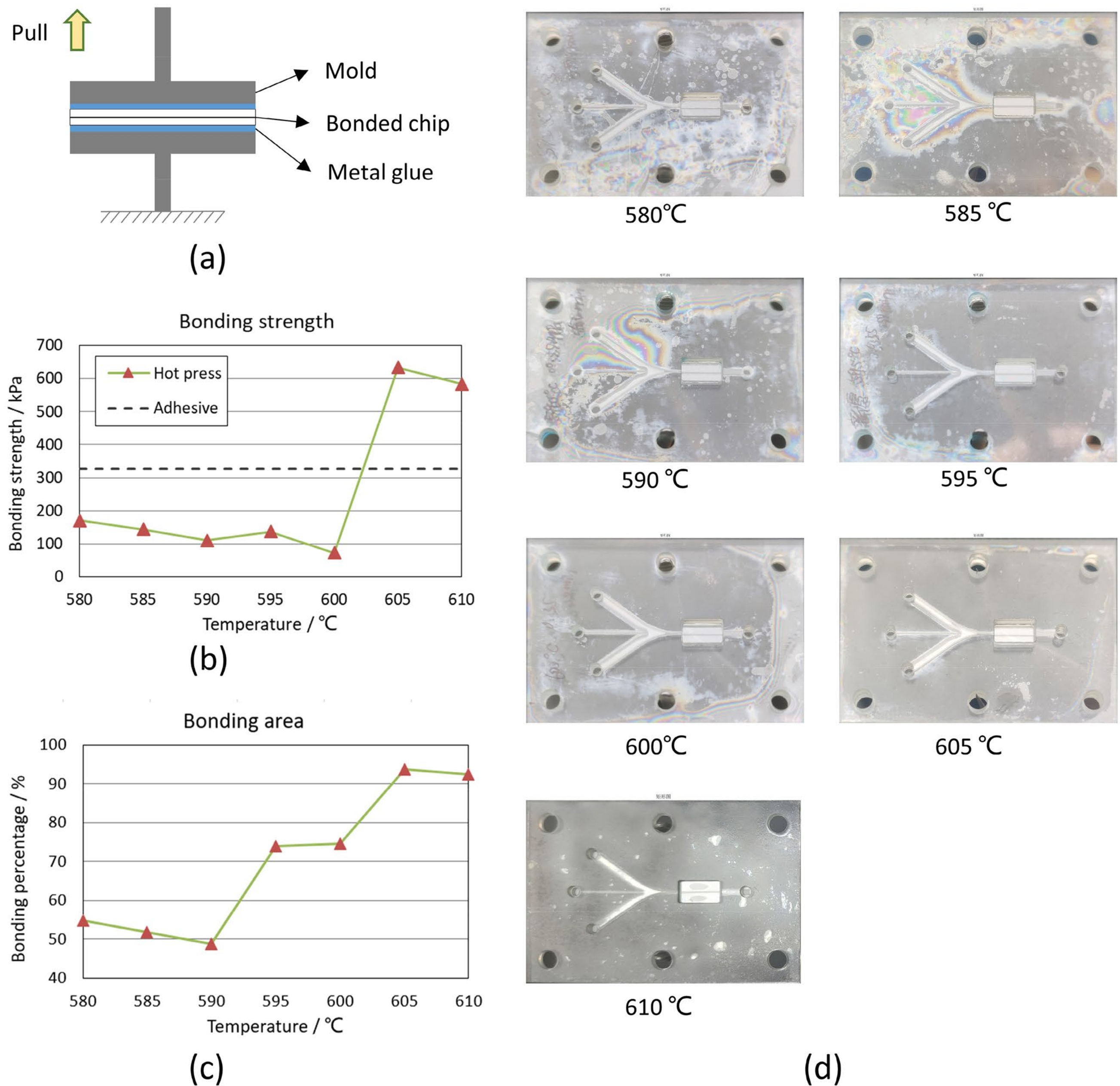

Fig. 2 Bonding strength test. **a** Setup of the tensile test. **b** The curve of bonding strength with temperature. **c** The relationship between the temperature and the bonded area. **d** Images of seven chips bonded at different temperatures

3.2 Microchannel deformation

For the bonding process, there is a basic requirement that the bonding process should not induce large deformation or damage to the microstructures. Generally speaking, in thermocompression bonding, tiny channel deformation is usually unavoidable, but for structures with dimensions in the order of tens or hundreds of microns, the deformation is relatively small at the level that will not affect the performance of the devices. Four chips bonded at 580 ℃, 590 ℃, 605 ℃, and 610 ℃ were measured, as shown in Fig. 3. we cut the microfluidic device and observed the cross-sections of the flow channels using a microscope (VHX-6000, Japan, Keyence).

The chip is cut from the middle position using the aforementioned laser processing machine. The cut line is shown by the dotted line in Fig. 3(a). The relationship between bonding temperature and channel height is shown in Fig. 3(b) and Fig. 3(c–d) is the microscopic images of the chip cross-section views at 580℃ and 610℃. At the temperature of 605 °C, the height of the flow channel is nearly the

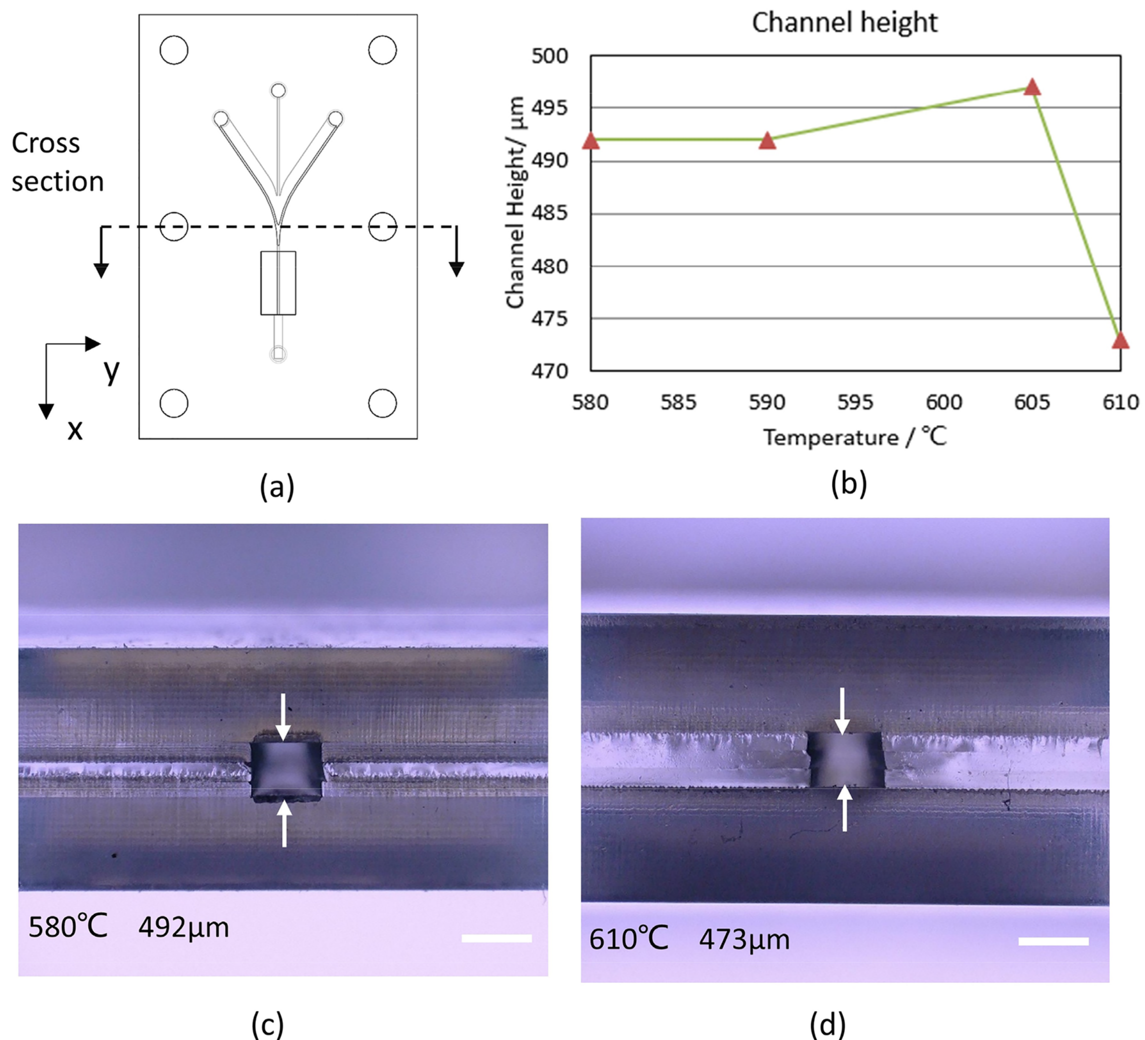

Fig. 3 Deformation test. **a** The cutting position on the chip. **b** The channel height at different temperatures. **c–d** The cross-section images of the chips bonded at 580 ℃ and 610 ℃. All the scale bars are 500 µm

same as those at lower temperatures (580 °C and 590 °C). When the temperature rises to 610 °C, the channel height of the three middle layer is vertically compressed by about 20 µm. This indicates that the optimal bonding temperature is 605 °C. At this temperature, both the sufficient bonding strength and small channel deformation can be met.

3.3 Sealing test

For microfluidic chips, it is necessary to ensure good sealing performance under certain liquid pressure. The bonding chips were further tested under high fluid pressure. As illustrated in Fig. 4(a), high-pressure liquid is injected into two inlets (the other two outlets marked by red crosses were blocked) and the real-time hydraulic pressure is measured by a gauge (CYYZ11, China, Star Sensor). As shown in Fig. 4(b), the observation windows comprise of three thin glass layer and is the most fragile part of the chip. The detailed structures of each layer are shown in Fig. 4(c), thus the hydraulic pressure at which the three middle 165 µm-thick glass layers in the observation window break and liquids leak is recorded to quantify the sealing performance.

The chip bonded at 605 ℃ was tested and the maximum pressure it can hold without damage is 0.25 MPa. In comparison, the typical liquid pressure is usually no more than 100 kPa (Patel et al. 2008; Glavan et al. 2013). It indicates that the sealing performance of this thermocompression bonding can satisfy most of the microfluidic chips.

3.4 Function test

Three-dimensional hydrodynamic focusing function of the five-layer chip is tested. 3D focusing plays a cardinal role

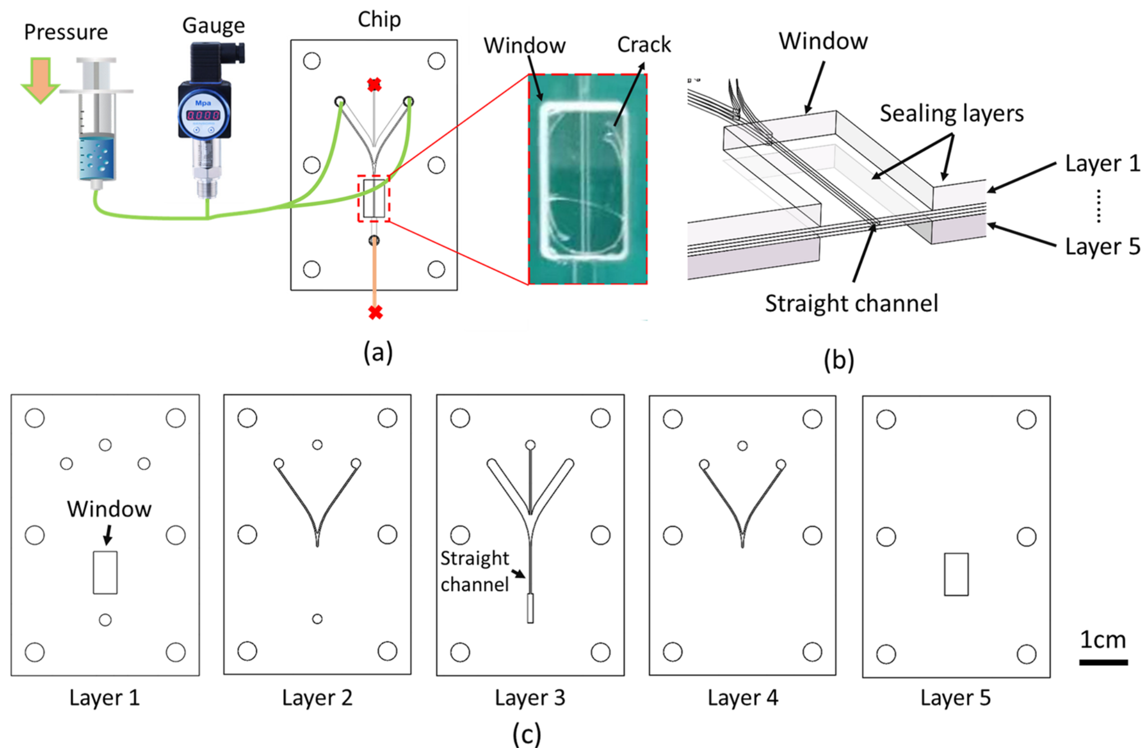

Fig. 4 **a** Setup of the sealing test. **b** The 3D structure of the observation window. **c** The structure of each layer of the five-layer microfluidics chip

for high-throughput analysis of bioparticles (Sundararajan et al. 2004), and the performance of a designed focusing microfluidic chip highly relies on the fabrication accuracy of its structure. In comparison, the same chip assembled using UV-curable adhesive (Zhao and You 2016) was measured.

The experiment was carried out with the same set-up in our previous work (Zhao and You 2015, 2016), as shown in Fig. 5(a). The 3D fluid conditions were visualized with confocal microscopy (Nikon Ti, Nikon, Japan). Rhodamine B aqueous solution (red) and sodium fluorescein aqueous solution (green) were respectively used as the sheath flow and the sample flow. The cross-sectional size of the straight channel is 165 μm × 300 μm. With the 3D hydrodynamic focusing by sheath flows, the sample flow was restricted to be a narrow stream along the channel centerline with the cross-sectional dimensions less than 20 μm × 30 μm. The 3D images were collected using a 10× objective with the 2 μm step for Z stacking. The focusing results of thermocompression and adhesive chips are shown in Fig. 5(b–c). The red represents the sample flow. The experiment proves that the sample flow is focused into a slender line. The cross-sectional dimensions of the focused sample flow were evaluated by the width of the half-maximum (FWHM) fluorescence intensity, as shown in Fig. 5(d–e). Under the same flow conditions (sample flow = 60 μL/min, sheath flow = 7200 μL/min), the sample flow dimensions of the thermocompression bonded chip were 17 μm × 27 μm, and those in the adhesive-bonded chip were 15 μm × 29 μm. It demonstrates that the chip fabricated by the work owns the same excellent performance as the chip fabricated by the complex adhesive method.

4 Discussion

Due to the physical and chemical inertness of glass and the structural complexity of multi-layer glass chips, the fabrication methods of multi-layer glass chips are usually complicated. Here we developed a simple fabrication method for multi-layer glass microfluidic chips, combining laser processing and thermocompression bonding technologies.

Table 1 listed the above glass processing and bonding methods. In all of these existing glass processing and bonding methods, we combined laser processing and thermocompression bonding based on the characteristics of multilayer microfluidic chips. The main advantages of our fabrication methods are less manual operation, simple and fast fabrication process. Limited manual operations are only required for laser cutting, chip cleaning, and aligning. The whole process does not need the high proficiency and expertise of the operators, benefiting the fabrication consistency. Laser cutting can effectively process single glass layers with the accuracy enough for microfluidic chips.

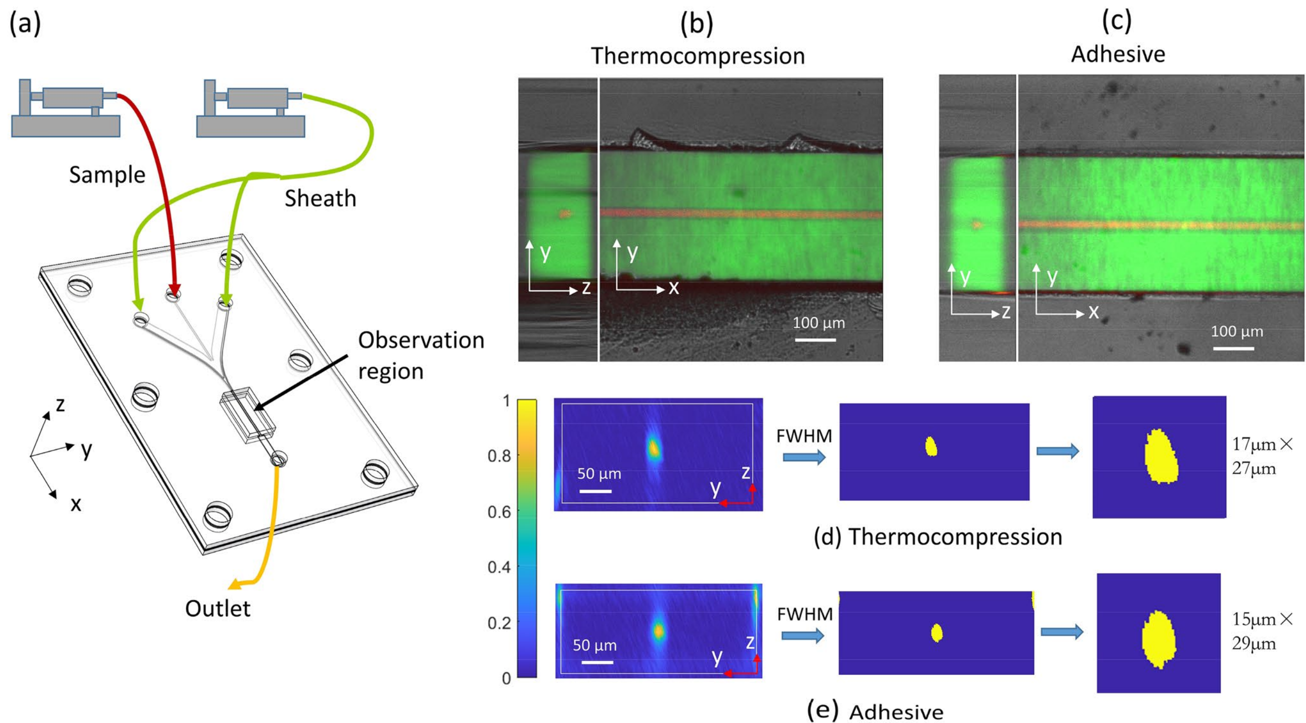

Fig. 5 Visualization of 3D focusing using confocal microscopy. **a** The schematic diagram of the confocal experiment. **b** The confocal images of the sample flow and sheath flow on the DC channel of the thermocompression bonded chip, images of x–y and y–z cross sections are given. **c** Confocal images of the UV-adhesive chip at the same position. **d–e** Measuring the cross-sectional dimensions of the focused sample flow of the thermocompression and adhesive boned chip, using the image processing method

Meanwhile, one-time alignment and thermocompression bonding realize the multi-layer glass chip bonding in a simple way.

This fabrication method can work for both multi-layer glass microfluidic chips, and the relatively simple glass microfluidics chips composed of two or three layers. Expect for multi-layer pure glass chips, this method can fabricate electrodes with laser cutting and integrate the electrodes into the microfluidic chip during the bonding process. The chip with electrodes is useful for cell sorting (Zhao and You 2018), cell impedance measurement (Iliescu et al. 2007), and droplet manipulation (Mazutis et al. 2013). Further improvements can also be made, for example, by introducing surface treatment to modify the glass surface to reduce the bonding temperature and the deformation of the chip, or combining wet etching or dry etching methods to extend this method to nanofluidic chips. In practical manufacture, the fabrication efficiency of thick glass sheets can be further improved combining other faster processing methods. For example, drillers can be used to produce positioning holes and windows, which have larger sizes and lower precision requirements. Based on the principle of this method, the mass production process for microfluidic glass chips will be developed.

5 Conclusion

This paper presents a simple, easy-to-operate fabrication method for multi-layer glass microfluidics chips which comprises laser cutting and thermocompression bonding. The laser cutting can process a single glass layer with the advantages of high efficiency and relatively high precision. The bonding is able to bond multi-layers of glass sheets at one time with a simple alignment and thermocompression bonding process. The optimal temperature and pressure are determined as 605 ℃ and 0.4 MPa, at which the deformation of the chips is neglectable. For demonstration, a five-layer 3D microfluidic focusing chip can be produced within 6 h (95 min for laser processing and 200 min for bonding), and the chip performance was tested to meet the requirements of use. In conclusion, this method can produce multi-layer glass microfluidic chips in simple ways, which is expected to reduce the fabrication cost of multi-layer glass microfluidic chips, realize the mass production, and wide application of multi-layer glass microfluidic chips.

Table 1 Summary of glass processing and bonding

	Method	Principle	Feature size	Processing speed
Glass processing	Wet etching	Using HF/HCl (10:1), HF, or HF/NH_4F as etchants Masking layers required	Limited by diffraction limit: ~ 0.5 µm for contact photo-lithography and ~ 0.3 µm for projection photo-lithography. (Iliescu et al. 2012)	Up to 7–8 µm/min
	Dry etching	Reactive ion etching, using SF_6, C_4F_8, CF_4 or CHF_3 Masking layers required		Up to 0.5–0.8 µm/min
	CNC micromachining	Micro milling or drilling	Limited by the size of milling tool	Fast when processing holes or windows
	Laser processing	Use ultrashort laser pulse to remove glass material	> 10 µm, limited by the laser spot size	Fast, depends on glass thickness and structural complexity
	Method	Principle	Applicability for multi-layer bonding	Pretreatment and time consuming
Glass bonding	Anodic bonding	Apply high temperature (420–530 ℃) and voltage (50–200 V) (Mrozek 2009) Intermediate layer required	Yes, but not reported	Chemical cleaning or ion cleaning, metal interlayer evaporation ~ 25 min for anodic bonding (Mrozek 2009)
	Surface pretreat bonding	Use sulfuric acid, piranha solution, or CF_4 plasma. etc. to clean and activate the surface	Yes	8–12 h (Jia et al. 2004) 15–20 h (Iles et al. 2007)
	Adhesive bonding	Use UV-curable adhesive to bond glass layers	No, need to bond one by one	Slow, require high expertise to avoid overflow of adhesive
	Thermo-compression bonding	Apply high temperature (> anneal point) and pressures to fuse the glass	Yes	Fast, one time alignment and one time bonding

Acknowledgements This work was supported by the fund for the Joint Project of Beijing (Beijing Municipal Commission of Education) and the National Natural Science of China (Grant Number: 61727813). The authors acknowledge Dr. XingZhe Yu from the School of Aerospace Engineering, Tsinghua University for his help in the bonding strength experiments.

References

Adam RC, David M, Camilo P, Gerard MOC (2015) Thin glass processing with various laser sources. Proc SPIE. Doi 10(1117/12):2077217

Akiyama Y, Morishima K, Kogi A, Kikutani Y, Tokeshi M, Kitamori T (2007) Rapid bonding of Pyrex glass microchips. Electrophoresis 28(6):994–1001. https://doi.org/10.1002/elps.200600437

Berthold A, Nicola L, Sarro PM, Vellekoop MJ (2000) Glass-to-glass anodic bonding with standard IC technology thin films as intermediate layers. Sens Actuators A 82(1):224–228. https://doi.org/10.1016/S0924-4247(99)00376-3

Chen X, Shen J, Zhou M (2016) Rapid fabrication of a four-layer PMMA-based microfluidic chip using CO2-laser micromachining and thermal bonding. J Micromech Microeng 26(10):107001. https://doi.org/10.1088/0960-1317/26/10/107001

Chen P, Li S, Guo Y, Zeng X, Liu B-F (2020) A review on microfluidics manipulation of the extracellular chemical microenvironment and its emerging application to cell analysis. Anal Chim Acta 1125:94–113. https://doi.org/10.1016/j.aca.2020.05.065

Daridon A, Fascio V, Lichtenberg J, Wütrich R, Langen H, Verpoorte E, de Rooij NF (2001) Multi-layer microfluidic glass chips for microanalytical applications. Fresenius J Anal Chem 371(2):261–269. https://doi.org/10.1007/s002160101004

Datta A, Gangopadhyay S, Temkin H, Pu Q, Liu S (2006) Nanofluidic channels by anodic bonding of amorphous silicon to glass to study ion-accumulation and ion-depletion effect. Talanta 68(3):659–665. https://doi.org/10.1016/j.talanta.2005.05.011

Du L, Allen MG (2018) Silica hermetic packages based on laser patterning and localized fusion bonding. 2018 IEEE Micro Electro Mech Syst. https://doi.org/10.1109/MEMSYS.2018.8346612

Du L, Allen MG (2019) CMOS compatible hermetic packages based on localized fusion bonding of fused silica. J Microelectromech Syst 28(4):656–665. https://doi.org/10.1109/JMEMS.2019.2913533

Gečys P, Dudutis J, RaČIukaitis G (2015) Nanosecond laser processing of soda-lime glass. J Laser Micro Nanoeng. https://doi.org/10.2961/jlmn.2015.03.0003

Glavan AC, Martinez RV, Maxwell EJ, Subramaniam AB, Nunes RMD, Soh S, Whitesides GM (2013) Rapid fabrication of pressure-driven open-channel microfluidic devices in omniphobic RF paper. Lab Chip 13(15):2922–2930. https://doi.org/10.1039/c3lc50371b

Huang Y, Liu S, Yang W, Yu C (2010) Surface roughness analysis and improvement of PMMA-based microfluidic chip chambers by CO2 laser cutting. Appl Surf Sci 256(6):1675–1678. https://doi.org/10.1016/j.apsusc.2009.09.092

Hwang J, Cho YH, Park MS, Kim BH (2019) Microchannel fabrication on glass materials for microfluidic devices. Int J Precis Eng Manuf 20(3):479–495. https://doi.org/10.1007/s12541-019-00103-2

Iles A, Oki A, Pamme N (2007) Bonding of soda-lime glass microchips at low temperature. Microfluid Nanofluid 3(1):119–122. https://doi.org/10.1007/s10404-006-0101-z

Iliescu C, Chen B, Miao J (2008) On the wet etching of Pyrex glass. Sens Actuators A 143(1):154–161. https://doi.org/10.1016/j.sna.2007.11.022

Iliescu C, Poenar DP, Carp M, Loe FC (2007) A microfluidic device for impedance spectroscopy analysis of biological samples. Sens Actuators B Chem 123(1):168–176. https://doi.org/10.1016/j.snb.2006.08.009

Iliescu C, Jing J, Tay FEH, Miao J, Sun T (2005) Characterization of masking layers for deep wet etching of glass in an improved HF/HCl solution. Surf Coat Technol 198(1):314–318. https://doi.org/10.1016/j.surfcoat.2004.10.094

Iliescu C, Taylor H, Avram M, Miao J, Franssila S (2012) A practical guide for the fabrication of microfluidic devices using glass and silicon. Biomicrofluidics 6(1):16505–1650516. https://doi.org/10.1063/1.3689939

Jang K-J, Suh K-Y (2010) A multi-layer microfluidic device for efficient culture and analysis of renal tubular cells. Lab Chip 10(1):36–42. https://doi.org/10.1039/B907515A

Jia ZJ, Fang Q, Fang ZL (2004) Bonding of glass microfluidic chips at room temperatures. Anal Chem 76(18):5597–5602. https://doi.org/10.1021/ac0494477

Jiao Z, Zhao J, Chao Z, You Z, Zhao J (2019) An air-chamber-based microfluidic stabilizer for attenuating syringe-pump-induced fluctuations. Microfluid Nanofluid 23(2):26. https://doi.org/10.1007/s10404-019-2193-2

Jin Y, Wang Y, Zhang X, Wang B (2020) Micro-milling of fused silica based on instantaneous chip thickness. J Mater Process Technol 285:116786. https://doi.org/10.1016/j.jmatprotec.2020.116786

Kalkowski G, Risse S, Zeitner U, Fuchs F, Eberhardt R, Tunnermann A (2014) (Invited) Glass-glass direct bonding. ECS Trans 64(5):3–11. https://doi.org/10.1149/06405.0003ecst

Kim S, Kim J, Joung YH, Ahn S, Koo C (2019) "Optimization of selective laser-induced etching (SLE) for fabrication of 3D glass microfluidic device with multi-layer micro channels. Micro Nano Syst Lett. https://doi.org/10.1186/s40486-019-0094-5

Kitamura R, Pilon L, Jonasz M (2007) Optical constants of silica glass from extreme ultraviolet to far infrared at near room temperature. Appl Opt 46(33):8118–8133. https://doi.org/10.1364/AO.46.008118

Lee C-Y, Chang C-L, Wang Y-N, Fu L-M (2011) Microfluidic mixing: a review. Int J Mol Sci. https://doi.org/10.3390/ijms12053263

Li JM, Liu C, Liu JS, Xu Z, Wang LD (2009) Multi-layer PMMA microfluidic chips with channel networks for liquid sample operation. J Mater Process Technol 209(15):5487–5493. https://doi.org/10.1016/j.jmatprotec.2009.05.003

Liu P, Lv Z, Sun B, Gao Y, Qi W, Xu Y, Chen L, Wang L, Ge C, Li S (2021) A universal bonding method for preparation of microfluidic biosensor. Microfluid Nanofluid 25(5):43. https://doi.org/10.1007/s10404-021-02445-8

Mazutis L, Gilbert J, Ung WL, Weitz DA, Griffiths AD, Heyman JA (2013) Single-cell analysis and sorting using droplet-based microfluidics. Nat Protoc 8(5):870–891. https://doi.org/10.1038/nprot.2013.046

Moraes C, Sun Y, Simmons CA (2009) Solving the shrinkage-induced PDMS alignment registration issue in multilayer soft lithography. J Micromech Microeng 19(6):065015. https://doi.org/10.1088/0960-1317/19/6/065015

Mrozek P (2009) Anodic bonding of glasses with interlayers for fully transparent device applications. Sens Actuators A 151(1):77–80. https://doi.org/10.1016/j.sna.2009.01.018

Mrozek P (2012) Glass-to-glass anodic bonding using TiNx interlayers for fully transparent device applications. Sens Actuators A 174:139–143. https://doi.org/10.1016/j.sna.2011.12.012

Pan YJ, Yang RJ (2006) A glass microfluidic chip adhesive bonding method at room temperature. J Micromech Microeng 16(12):2666–2672. https://doi.org/10.1088/0960-1317/16/12/020

Park JH, Lee NE, Lee J, Park JS, Park HD (2005) Deep dry etching of borosilicate glass using SF6 and SF6/Ar inductively coupled

plasmas. Microelectron Eng 82(2):119–128. https://doi.org/10.1016/j.mee.2005.07.006
Patel JN, Kaminska B, Gray BL, Gates BD (2008) PDMS as a sacrificial substrate for SU-8-based biomedical and microfluidic applications. J Micromech Microeng 18(9):095028. https://doi.org/10.1088/0960-1317/18/9/095028
Sano H, Kazoe Y, Morikawa K, Kitamori T (2020) Implementation of a nanochannel open/close valve into a glass nanofluidic device. Microfluid Nanofluid 24(10):78. https://doi.org/10.1007/s10404-020-02383-x
Su T, Cheng K, Sun Y (2019) Fast packaging of glass-based microfluidic chip using adhesive polyurethane material. Microsyst Technol 25(11):4399–4403. https://doi.org/10.1007/s00542-019-04516-x
Sundararajan N, Pio MS, Lee LP, Berlin AA (2004) Three-dimensional hydrodynamic focusing in polydimethylsiloxane (PDMS) microchannels. J Microelectromech Syst 13(4):559–567. https://doi.org/10.1109/JMEMS.2004.832196
Sung-Il K, Jeongtae K, Chiwan K, Yeun-Ho J, Jiyeon C (2018) Rapid prototyping of 2D glass microfluidic devices based on femtosecond laser assisted selective etching process. SPIE, Proc. https://doi.org/10.1117/12.2291160
Webb AP, Houghton AJ, Townsend PD (1976) Changes in the chemical stability of ion-implanted silica glass. Radiat Eff 30(3):177–182. https://doi.org/10.1080/00337577608233060
Wu C-Y, Liao W-H, Tung Y-C (2011) Integrated ionic liquid-based electrofluidic circuits for pressure sensing within polydimethylsiloxane microfluidic systems. Lab Chip 11(10):1740–1746. https://doi.org/10.1039/C0LC00620C
Wu Y, Qian X, Zhang M, Dong Y, Sun S, Wang X (2018) Mode transition of droplet formation in a semi-3D flow-focusing microfluidic droplet system. Micromachines. https://doi.org/10.3390/mi9040139
Xiong S, Chen X (2021a) Numerical simulation of three-dimensional passive micromixer with variable-angle grooves and baffles. Surf Rev Lett 28(05):2150037. https://doi.org/10.1142/S0218625X21500372
Xiong S, Chen X (2021b) Numerical study of a three-dimensional electroosmotic micromixer with Koch fractal curve structure. J Chem Technol Biotechnol 96(7):1909–1917. https://doi.org/10.1002/jctb.6711
Xiong S, Chen X, Chen H, Chen Y, Zhang W (2021) Numerical study on an electroosmotic micromixer with rhombic structure. J Dispersion Sci Technol 42(9):1331–1337. https://doi.org/10.1080/01932691.2020.1748644
Xu Y, Wang C, Li L, Matsumoto N, Jang K, Dong Y, Mawatari K, Suga T, Kitamori T (2013) Bonding of glass nanofluidic chips at room temperature by a one-step surface activation using an O2/CF4 plasma treatment. Lab Chip 13(6):1048–1052. https://doi.org/10.1039/c3lc41345d
Yang J, Tu R, Yuan H, Wang Q, Zhu L (2021) Recent advances in droplet microfluidics for enzyme and cell factory engineering. Crit Rev Biotechnol. https://doi.org/10.1080/07388551.2021.1898326
Zhao J, You Z (2015) Microfluidic hydrodynamic focusing for high-throughput applications. J Micromech Microeng 25(12):125006. https://doi.org/10.1088/0960-1317/25/12/125006
Zhao J, You Z (2016) A microflow cytometer with a rectangular quasi-flat-top laser spot. Sensors (basel, Switzerland) 16(9):1474. https://doi.org/10.3390/s16091474
Zhao J, You Z (2018) Spark-generated microbubble cell sorter for microfluidic flow cytometry. Cytometry A 93(2):222–231. https://doi.org/10.1002/cyto.a.23296

Publisher's Note Springer Nature remains neutral with regard to jurisdictional claims in published maps and institutional affiliations.